An Experimental Investigation on Refrigerant-Water Flow Distribution and Local Heat Transfer Performance in Plate Heat Exchangers

by C.-Y. Yang, Y.-H. Lin and T.-W. Hsu

Graduate Institute of Energy Engineering, National Central University, 320 Jhongli, Taiwan, *cyyang@ncu.edu.tw*

Abstract

This study provides an experimental investigation on the local heat transfer performance of refrigerant-water heat transfer in a plate heat exchanger. The Infrared Thermography was used for measuring the surface temperature on the water-side plate. The local heat transfer coefficient was obtained by integrating the water flow rate and temperature difference between the adjacent points on the plate. The test results show that saturated and superheated areas can be clearly observed by the IR image. In the intersection of these two regions, a drastically water temperature decrease was observed. This is attributed to the high heat transfer coefficient of evaporation and high temperature difference between water and refrigerant and therefore high heat transfer rate.

1. Introduction

A plate heat exchanger is made by combing several corrugated stainless plates. The hot and cold working fluids pass through the channels between adjacent plates and exchange heat through the plate. In comparing to the shell-and-tube heat exchangers, the plate heat exchangers provide high effectiveness at very compact size. It is commonly used as evaporators or condensers in air-condition and refrigeration systems because of its compactness and high heat transfer performance. The hot and cold side fluids are usually in counter flow arrangement to minimize the approach temperature difference.

Even though the plate heat exchangers are popularly used in industries, but only very few experiments about their fluid dynamics and the local heat transfer have been published in the literature. Gaiser and Kottke [1] used the ammonia absorption method to study flow phenomena and local heat transfer coefficients of PHE plates with various pitch angles and corrugation wavelengths in a wind tunnel. They determined the heat transfer coefficients from the light reflectance of the absorption paper samples and presented a surface map of Nusselt numbers. Stasiek et al. [2] and Ciofalo et al. [3] investigated the distributions of local Nusselt numbers on cross-corrugated surfaces. They used the thermochromic liquid crystals (TLC) method on model structures in a wind tunnel to measure their heat transfer performance. Their results include Nusselt number maps of unitary cells of the cross-corrugated structure for various angles and Reynolds numbers.

Djordjevic and Kabelac [4] and Živković et al. [5] investigated the quasi-local evaporation heat transfer coefficient of the refrigerant R-134a and Ammonia in a vertical plate heat exchanger by inserting thermocouples through the gasket between two plates to measure the local fluid and plate temperatures. The temperature readings allowed for local energy balances of volume segments along the plate, which finally resulted in quasi-local heat transfer coefficients as a function of vapor quality on the refrigerant side of the PHE.

Freund and Kabelac [6] developed a method for the measurement of local convective heat transfer coefficients from the outside of a heat transferring wall. The technique relies first on experimental data of the phase lag of the outer surface temperature response to periodic heating, and second on a simplified numerical model of the heat exchanger wall to compute the local heat transfer coefficients from the processed data. Their results from the plate heat exchanger show a very distinct pattern of the heat transfer coefficients, with the minimum heat transfer at the crossing points of the corrugated structures and lines of local maxima along the corrugations. With increasing Reynolds number, the ratio of the maxima to the minima decreases and the pattern is less defined, while an area of minimum convection grows behind the crossing points. The mean values are in good agreement to literature data. Measurements of an entire plate were carried out to investigate the macro scale flow pattern and did not find significant mal-distribution of the flow field.

Flow mal-distribution may degrade heat exchanger performance significantly especially for the low aspect ratio heat exchangers like plate heat exchangers. Measurement of local heat transfer coefficient is the most direct way to realize the flow distribution and heat transfer performance for a heat exchanger. This study developed a direct method to investigate the local heat transfer performance of refrigerant-water heat transfer in a plate heat exchanger by the method of Infra-Red Thermography. It provided an efficient method for further improving the heat transfer performance of plate heat exchangers.

2. Experimental method

2.1 Test section

The test section was made by brazing four chevron corrugated thin stainless steel plates to form a three flow passages (one refrigerant and two water flow passages) plate heat exchanger. Two thick stainless steel flat plates were brazed on both side of the heat exchanger for enhancing its strength. Two square windows were cut from the front end plate, as shown in Figure 1, for Infrared image observation.

Figure 2 shows geometric parameters and flow arrangement of the test heat exchanger. Refrigerant R-410A was used as the working fluid which flowing through the central passage of the test section upwardly while water flew through the outer two side flow passages downwardly to form a counter flow arrangement heat exchanger. Detail dimensions of the test plate heat exchanger are listed in Table 1.
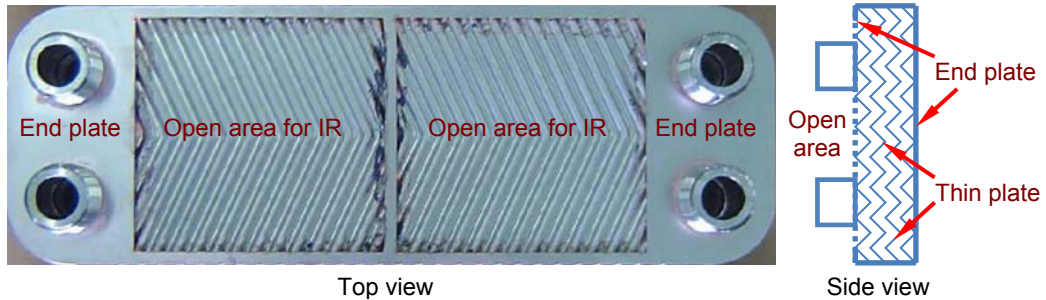

Top view   Side view

Fig. 1. *Schematic diagram of the test section*
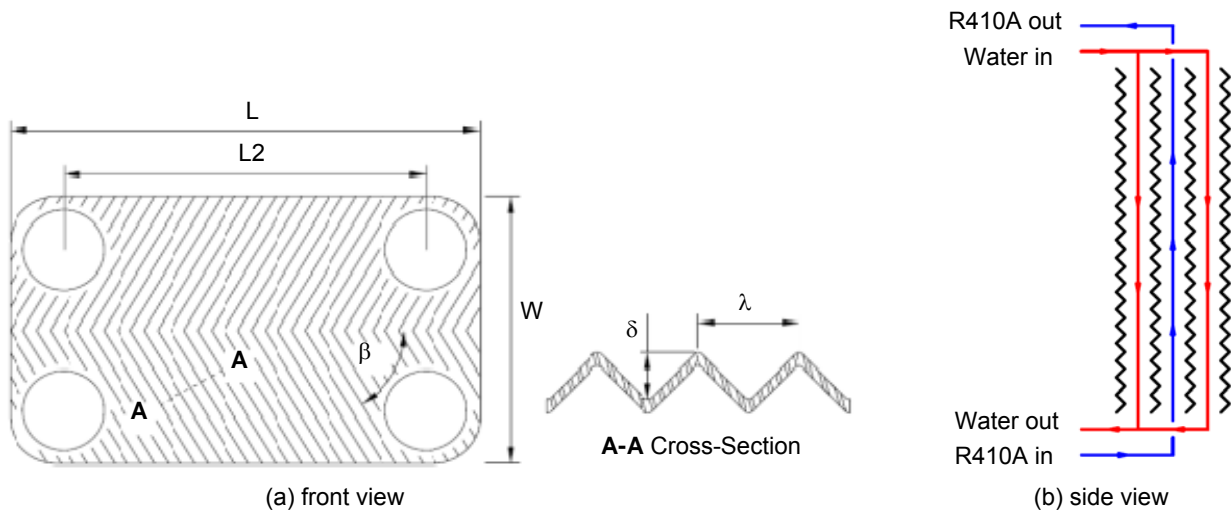

(a) front view   (b) side view

Fig. 2. *Geometric parameters and flow arrangement of the test heat exchanger*

Table 1. *Detail dimensions of test heat exchanger*

Plate length (L)	300 mm
Plate width (W)	102 mm
Longitudinal distance between ports (L2)	250 mm
Plate thickness (t)	0.4 mm
Amplitude of chevron passage (δ)	2 mm
Wave length (λ)	7 mm
Chevron angle (β)	65°
Hydraulic diameter of chevron passage (D_h)	4 mm
Heat transfer area (A = W x L2), (plate projected area, double sides)	0.051 m^2
Cross section area of single Passage (A_c)	0.000204 m^2
Cross section area of the window for IR image	90 x 90 cm^2

2.2 Experimental system

The schematic diagram of the experimental system is shown in Figure 3. It consists of three main loops, i.e., a refrigerant loop, a cooling water loop and a chill water-glycol loop.

2.2.1 Refrigerant loop

The refrigerant system was modified from a commercial chill water unit. As shown in Figure 3, refrigerant R-410A moved by an inverter controlled variable speed compressor to the condenser. It condensed in the condenser to high pressure liquid and flew through the expansion valve. A bypass was setup in the loop prior to the expansion valve. Part of the liquid refrigerant flew through the bypass and another expansion valve to become two-phase liquid-vapor flow and evaporated by the chill water in the test section. The rest refrigerant flew through its original loop into the evaporator. The vaporized refrigerant from the test section and the evaporator then merged together and flew into the compressor to complete a close cycle. The refrigerant flow rate was controlled independently by the variable speed compressor. The heat transfer rate and the refrigerant operation conditions were adjusted by the opening of the expansion valve and the cooling water and chill water temperatures and flow rates.

2.2.2 Cooling water loop

The cooling water for the condenser of the refrigerant system was provided by a large thermostat reservoir. The temperature controlled cooling water was pumped from that reservoir to the condenser. It absorbed heat from the condensing refrigerant and then flew into the evaporator to heat the evaporating refrigerant and finally flew back to the reservoir. The cooling water loop for condenser and the heating water loop for evaporator were connected together to recovery heat through these two processes.

2.2.3 Chill water-glycol loop

The chill water-glycol loop was used for heating the refrigerant in the test section. Chill water moved by a variable speed centrifugal pump from a low temperature reservoir and entered the test section at a known temperature and flow rate. It evaporated the refrigerant flowing through the other side of the test section. The chilled water left the test section and went back to the reservoir to complete a close loop. A preheater and a gear flow meter were installed between the pump and the test section to adjust the water temperature and measure water flow rate respectively.
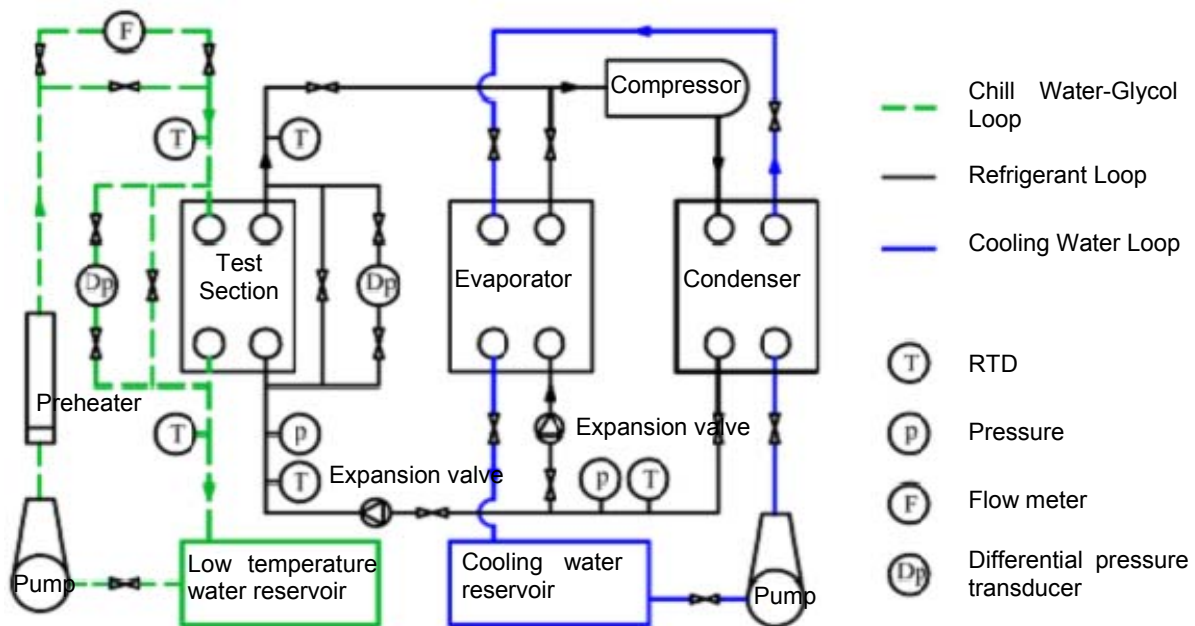

Fig. 3. *Schematic diagram of the test system*

2.3 Data reduction

Since the plate is thin and the test heat exchanger was well insulated during the test, the local water temperature beneath the measuring point, T_{wn} is approximately equal to the plate temperature at the point, T_n measured by the IR thermography. This has been varied from the test results by Djordjevic and Kabelac [3] especially for the area along the corrugations which far away from the crossing points of the corrugated structures.

As shown in Figure 4, plate surface temperatures were measured at the convex points along the corrugations and equal size control volumes were defined as the nearby area of the temperature measure points. For the control volume between two adjacent measuring points, from energy balance, the refrigerant side heat transfer rate equals to the water side heat transfer rate, $q_n = q_{rn} = q_{wn}$. The water side heat transfer rate, q_{wn} between these two points is the product of the local water flow rate, m_{wn} and the water temperature difference at these two points, T_{wn}, and T_{wn+1}:

$$q_n = q_{rn} = q_{wn} = m_{wn} c_{pw} (T_{wn} - T_{wn+1}) \tag{1}$$

The local water flow rate, m_{wn} can be obtained from the analysis by Wu et al. [7]. Thus the local heat transfer coefficient, h_n thus can be calculate as:

$$h_n = \frac{q_n}{\Delta A_n \Delta T_{lmn}}$$ (2)

Where ΔA_n is the heat transfer area of the control volume, the logarithmic mean temperature difference is defined as:

$$\Delta T_{lmn} = \frac{(T_{sat} - T_{wn}) - (T_{sat} - T_{wn+1})}{\ln\left(\frac{(T_{sat} - T_{wn})}{(T_{sat} - T_{wn+1})}\right)}$$ (3)

The refrigerant saturation temperature, T_{sat} is evaluated from its saturation pressure. The Reynolds number and Nusselt number are defined as:

$$Re_r = \frac{Gd_h}{\mu}$$ (4)

$$Nu_r = \frac{hd_h}{k_l}$$ (5)

Where G is the refrigerant mass flux, $G = m/A_c$, A_c is the flow passage cross-section area.

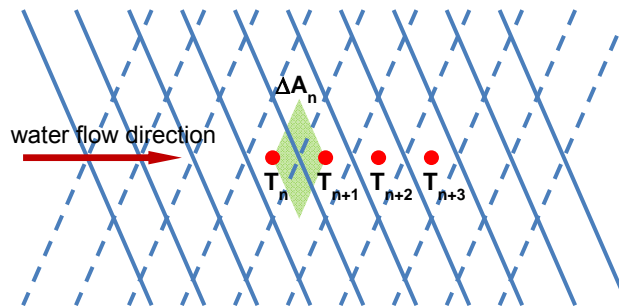*Fig. 4. Plate temperature measuring points*

3. Results and discussion

Figure 5 shows the test plate surface IR image at Re = 651 and exit superheat of 5 ^{o}C. The temperature of three flow paths along the plate (A, B and C) was also shown in the Figure. Two different heat transfer regions, i.e. saturated and superheated areas are clearly observed. A schematic diagram of temperature variation during heat transfer process is shown in Figure 6. In the saturated region, two-phase refrigerant kept at its saturation temperature corresponding to its saturation pressure. Water temperature decreased gradually along its flow direction which in reverse of the refrigerant flow. The surface temperature at the convex region along the corrugations is significantly higher than that at the concave crossing point of the corrugated structure. In the superheated region, refrigerant vapor temperature increase along its flow. However, owing to its low heat transfer coefficient, the water temperature decrease does not as large as refrigerant vapor does. In the intersection of saturated and superheated region, a drastically water temperature decrease was observed. This is attributed to the high heat transfer coefficient of evaporation and high temperature difference between water and refrigerant and therefore high heat transfer rate.

Figure 7 shows plate surface IR image and temperature variation for refrigerant flow without exit superheat. The general temperature distribution of this figure is similar to that of Figure 5 except the high temperature area is much smaller in Figure 7. Since the measured exit condition is the average refrigerant flow condition, there still be a superheat area at the center part of the exit even though the measured average exit superheat is 0 ^{o}C.

The local plate temperature was measured at the convex points along the corrugations. Figure 5 shows one of the measuring points along the centerline of the plate. The local heat transfer coefficient at the center measuring point of the plate for various refrigerant Reynolds number by the previous described method is shown in Figure 8. It increases with increasing Reynolds number and reasonably agrees with conventional theory. Further detail local heat transfer performance for late heat exchangers can be obtained by this method.
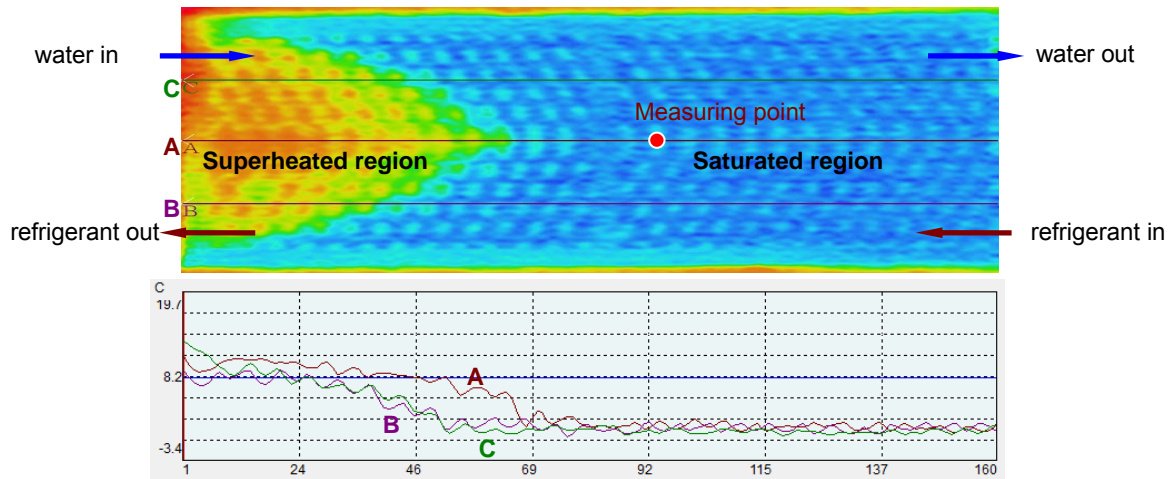
Fig. 5. *Temperature distribution alone flow path A, B and C, $\Delta T_{sat} = 5\,^{o}C$*
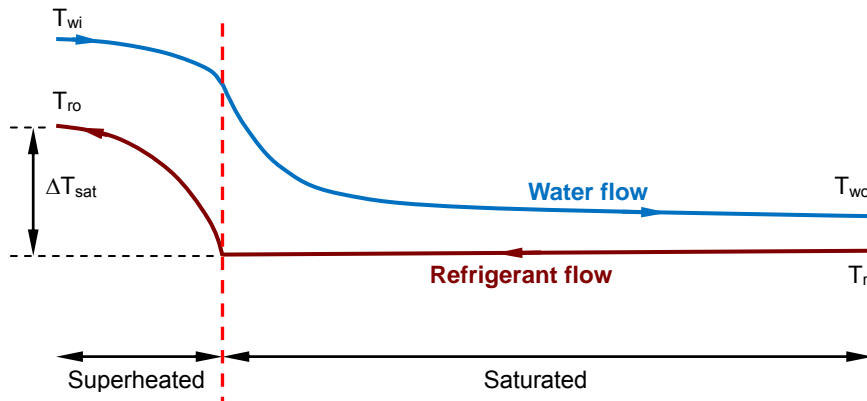

Fig. 6. *Schematic diagram of temperature variation during heat transfer process*
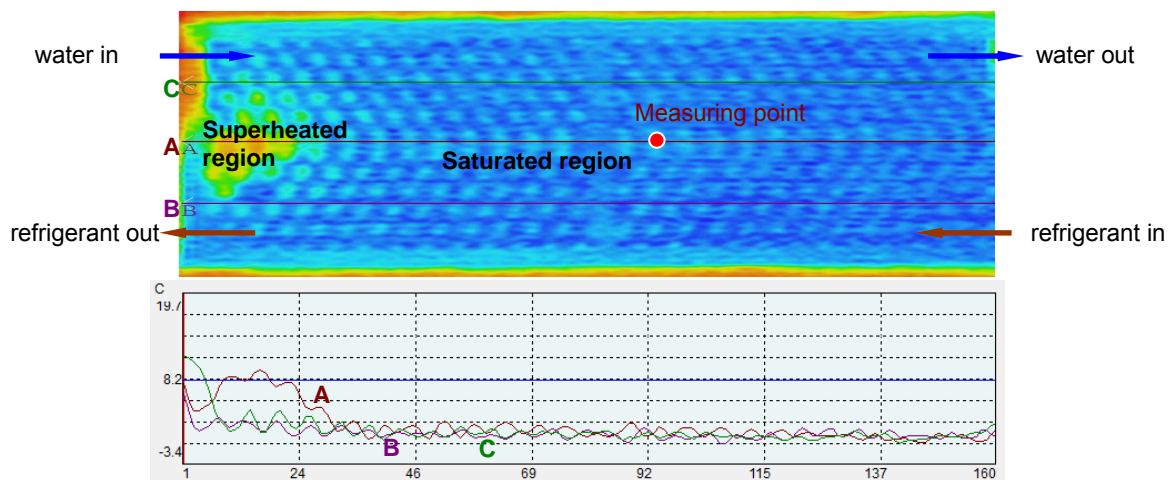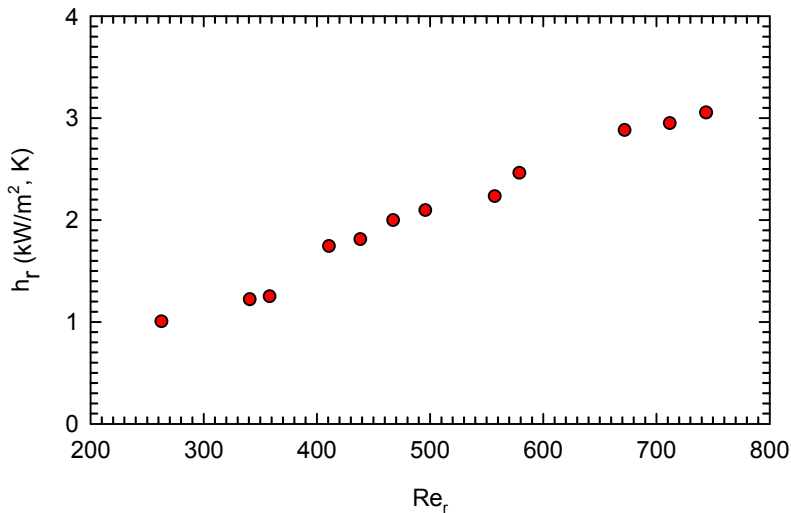

Fig. 7. *Temperature distribution alone flow path A, B and C, $\Delta T_{sat} = 0\,^{o}C$*

Fig. 8. *Local heat transfer coefficient at the center point of the plate*

REFERENCES

[1] Gaiser, G. and Kottke, V., "Flow phenomena and local heat and mass transfer in corrugated passages," Chemical Engineering Technology, vol. 12, pp. 400–405, 1989.

[2] Stasiek, J.A., Collins, M.W., Ciofalo, M. and Chew, P.E., "Investigation of flow and heat transfer in corrugated passages Part I," International Journal of Heat and Mass Transfer, vol. 39, no. 1, pp. 149–164, 1996.

[3] Ciofalo, M., Stasiek, J.A. and Collins, M.W., "Investigation of flow and heat transfer in corrugated passages Part II," International Journal of Heat and Mass Transfer, vol. 39, no. 1, pp.165–192, 1996.

[4] Djordjevic, E., and Kabelac, S., "Flow Boiling of R134a and Ammonia in a Plate Heat Exchanger, International Journal of Heat and Mass Transfer," Vol. 51, pp. 6235–6242, 2008.

[5] Živković, E., Kabelac, S. and Šerbanović, S., "Local heat transfer coefficients during the evaporation of 1,1,1,2-tetrafluoroethane (R-134a) in a plate heat exchanger," Journal of Serbian Chemical Society, vol. 74, no. 4, pp. 427–440, 2009.

[6] Freund, S. and Kabelac, S., "Investigation of local heat transfer coefficients in plate heat exchangers with temperature oscillation IR thermography and CFD," International Journal of Heat and Mass Transfer, vol. 53, pp. 3764–3781, 2010.

[7] Wu, J.-C., Lin, Y.-H., Chu, Y.-C., Meng, F.-Y. and Yang, C.-Y. Yang, "Experimental and Numerical Analysis on the Flow Distribution in a Plate Heat Exchanger with Inlet Distributor," Sixth International Conference on Thermal Engineering: Theory and Applications May 29-June 1 2012, Istanbul, Turkey.